

Supporting Information

Self-Assembly of Cyclic Nanoscale Polyoxotungstate Tellurim Embedded Cluster ‘Squares’: From Clusters to Emergent Microtubular Materials

Jing Gao, Jun Yan, Scott G. Mitchell, Haralampos N. Miras, Antoine G. Boulay,
De-Liang Long*and Leroy Cronin*

WestCHEM, School of Chemistry, The University of Glasgow, Glasgow G12 8QQ, U.K.

E-mail: deliang.long@glasgow.ac.uk, lee.cronin@glasgow.ac.uk

I Table S1. Crystal Data and Structure Refinement Details for compounds 1, 2 and 3

	(1)	(2)	(3)
chemical formula	C ₁₂ H ₁₅₄ N ₆ Na ₁₈ O ₁₆₅ Te ₈ W ₂₈	H ₇₄ Na ₂₆ O ₁₅₂ Te ₉ W ₂₈	H ₉₀ Na ₂₈ O ₁₆₃ Te ₁₀ W ₂₈
formula mass	9605.83	9405.57	9766.24
Cryst. Syst.	Orthorhombic	Triclinic	Monoclinic
space group	Pmmn	P-1	C2/c
T (K)	150	150	150
a (Å)	21.1146(6)	19.3418(8)	34.8730(1)
b (Å)	32.0756(10)	21.0639(10)	18.6557(3)
c (Å)	12.6836(4)	22.8563(11)	27.5438(8)
α(deg)	90	104.296(4)	90
β (deg)	90	91.843(4)	105.384(4)
γ (deg)	90	92.426(4)	90
V(Å ³)	8590.1(5)	9006.8(7)	17277.4(6)
Z	2	2	4
μ (mm ⁻¹)	45.664	44.873	20.397
total data collected	20760	41008	56442
unique data	7091	19584	16202
R _{int}	0.0583	0.0679	0.0631
R ₁	0.0475	0.0719	0.0485
wR ₂ [I > 2σ(I)]	0.1187	0.1659	0.1205
R ₁ (all data)	0.0737	0.1443	0.0781
wR ₂ (all data)	0.1317	0.2026	0.1273

Note: Compound **1** could be also obtained as single crystals of K₂₄[W₂₈Te₈O₁₁₂]•65H₂O **1'** by using a similar method as follows: TeO₂ (0.10 g, 0.62 mmol) was dissolved in 2 mL 2.5M aqueous KOH, which was then added to a solution of K₂WO₄ (1.00 g, 3.07 mmol) in 30 mL water and the pH of solution adjusted to ca. 7.0 with 37 % hydrochloric acid. The procedure is then completed as per the synthesis of

compound **1**. Crystal data for compound $K_{24}[W_{28}Te_8O_{112}] \cdot 65H_2O$ **1'**: monoclinic, $P2_1/n$, $a = 19.7207(4)$ Å, $b = 37.8627(11)$ Å, $c = 22.6396(4)$ Å, $\beta = 104.374(2)^\circ$, $V = 16375.3(6)$ Å³, $Z = 4$, $T = 150$ K, 131331 reflections measured, 31020 unique ($R_{\text{int}} = 0.1236$) which were used in all calculations. Final $R_1 = 0.0681$ and $wR_2 = 0.1452$ (all data).

Compound **2** has been obtained as single crystals of $Na_{27}[W_{28}Te_9O_{115}]Cl \cdot 71H_2O$ **2'** by using the same method to synthesize compound **2** but using HCl to adjust the pH of solution, resulting in one more chloride anion in the molecular formula. Crystal data for compound $Na_{27}[W_{28}Te_9O_{115}]Cl \cdot 71H_2O$ **2'**: monoclinic, $C2/m$, $a = 32.5176(6)$ Å, $b = 20.9370(3)$ Å, $c = 27.2721(4)$ Å, $\beta = 102.804(2)^\circ$, $V = 18105.7(5)$ Å³, $Z = 4$, $T = 150$ K, 47653 reflections measured, 12230 unique ($R_{\text{int}} = 0.0614$) which were used in all calculations. Final $R_1 = 0.0566$ and $wR_2 = 0.1618$ (all data).

II Inter-molecular interactions existing in compounds **2** and **3**

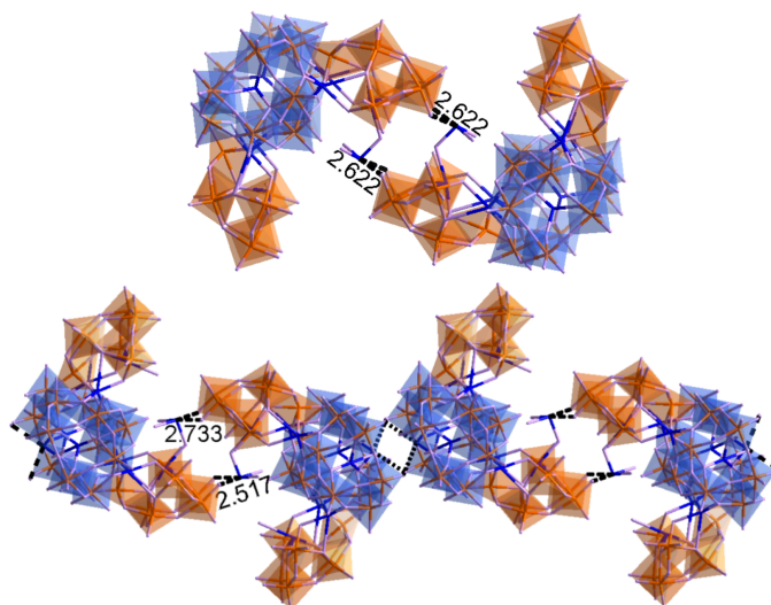


Fig. S2.1 Structures forming by inter-molecular interactions of compound **2** (top) and compound **3** (bottom) (the value marked is the according distance between Te and O). All cations and solvent water molecules are omitted for clarity.

III Thermogravimetric Analysis

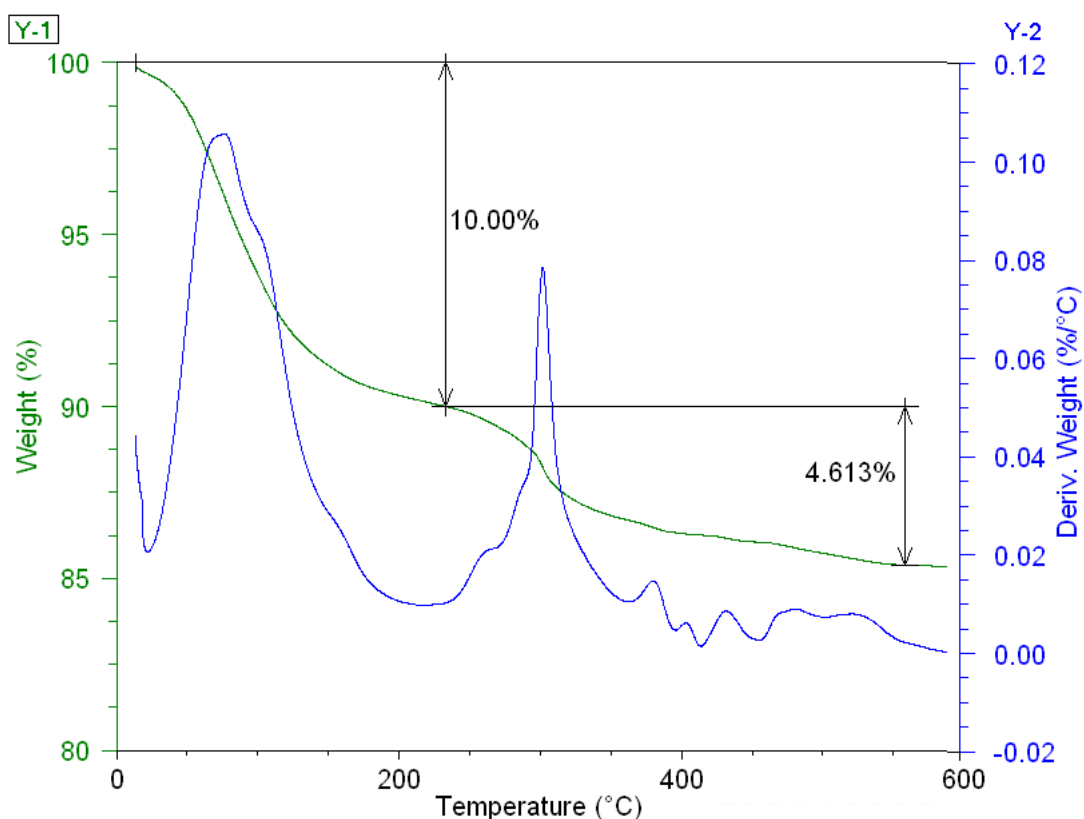


Figure S3.1 Thermogravimetric analysis of $(\text{C}_2\text{H}_8\text{N})_6\text{Na}_{18}[\text{W}_{28}\text{Te}_8\text{O}_{112}] \cdot 53\text{H}_2\text{O}$ (1)

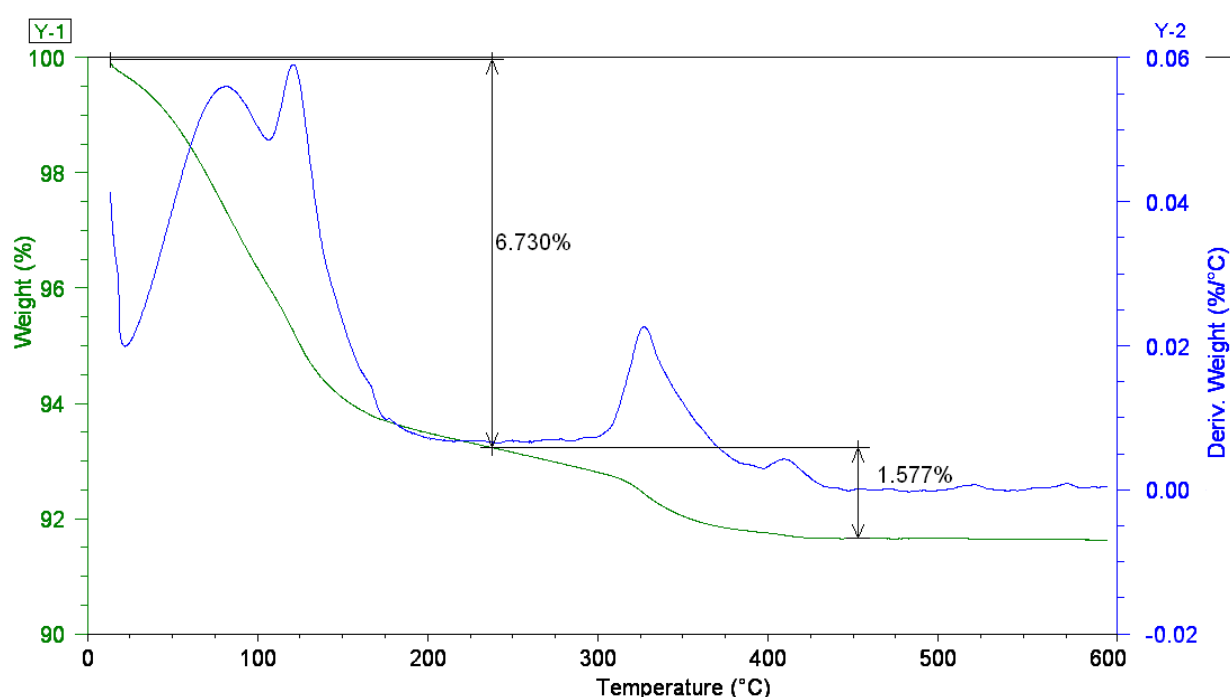


Figure S3.2 Thermogravimetric analysis of $\text{Na}_{26}[\text{W}_{28}\text{Te}_9\text{O}_{115}] \cdot 37\text{H}_2\text{O}$ (2)

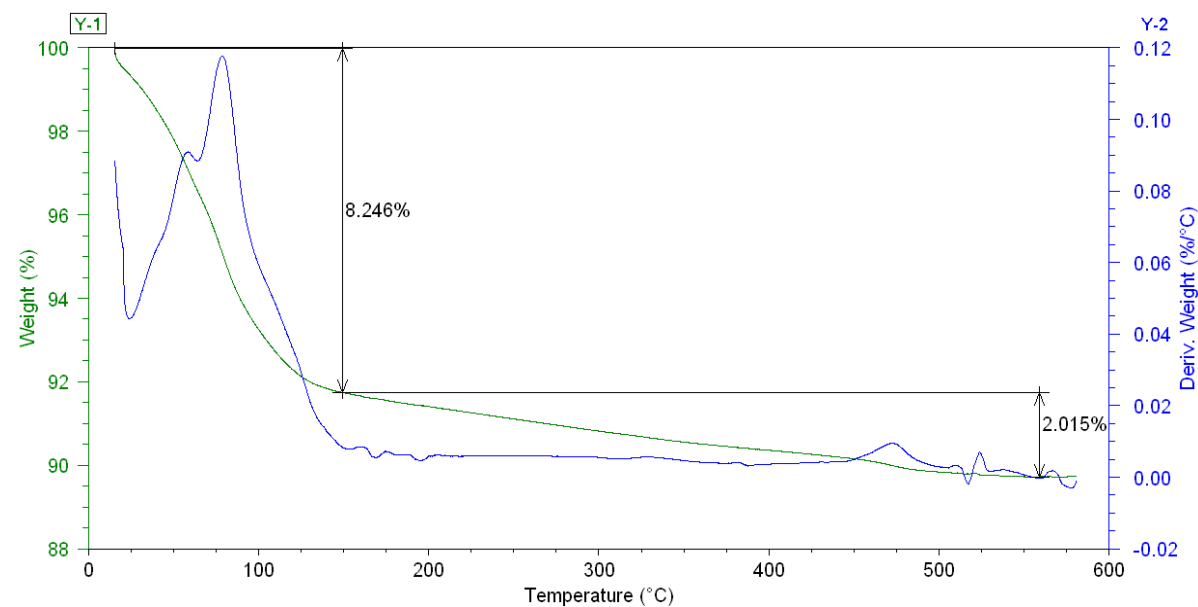


Figure S3.3 Thermogravimetric analysis of $\text{Na}_{28}[\text{W}_{28}\text{Te}_{10}\text{O}_{118}] \cdot 45\text{H}_2\text{O}$ (**3**)

IV Cryospray Mass Spectroscopic of compounds 1, 2 and 3

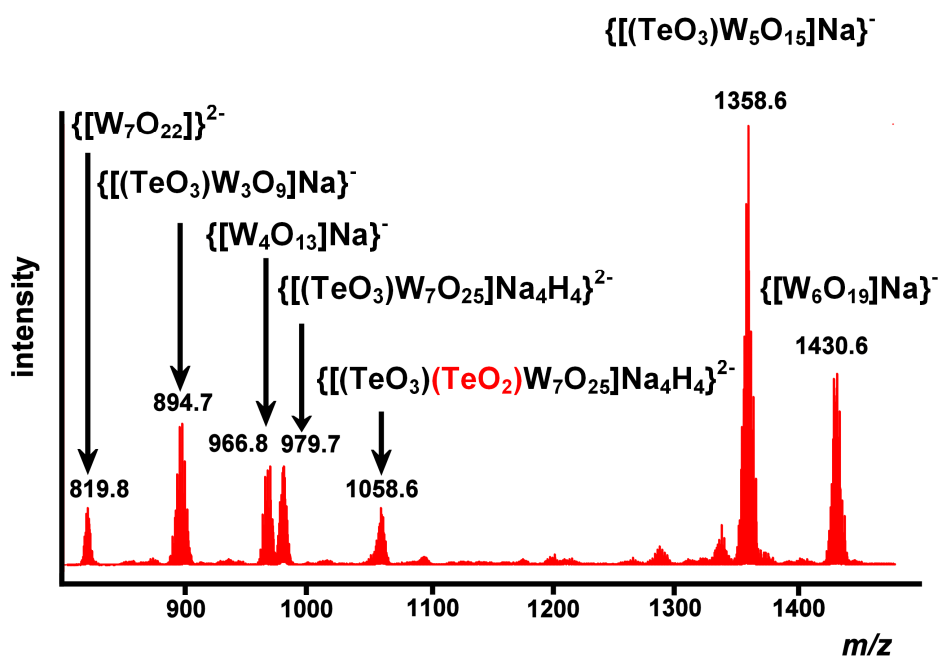


Figure S4.1 Mass Spectra data of $(C_2H_8N)_6Na_{18}[W_{28}Te_8O_{112}] \cdot 53H_2O$ (**1**) in a 50:50 water : acetonitrile mixture, transferred to the gas phase by electrospray ionisation (ESI). The spectrum shows the presence of key ions in the gas phase; in particular: $\{[W_7O_{22}]\}^{2-}$ (m/z 819.8); $\{[(TeO_3)W_3O_9]Na\}^-$ (m/z 894.7); $\{[(TeO_3)W_7O_{25}]H_4Na_4\}^{2-}$ (m/z 979.7); $\{[(TeO_3)W_5O_{15}]Na\}^-$ (m/z 1358.6) and $\{[W_6O_{19}]Na\}^-$ (m/z 1430.6). One of the most important features relates to the presence of one quarter unit of **1** including the TeO_2 linker: $\{[(TeO_3)(TeO_2)W_7O_{25}]H_4Na_4\}^{2-}$ (m/z 1058.6).

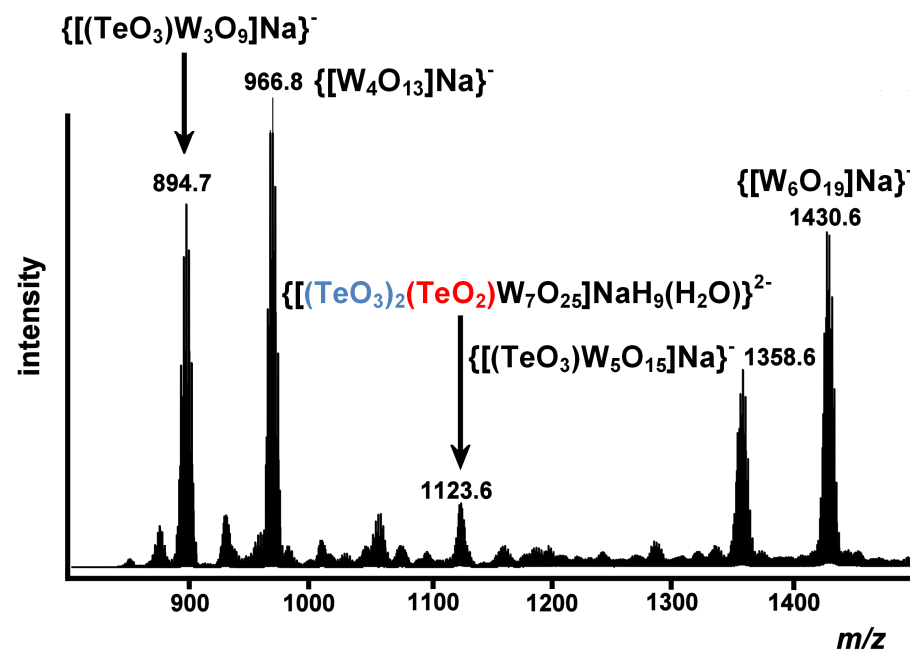


Figure S4.2 Mass Spectra data of $Na_{26}[W_{28}Te_9O_{115}] \cdot 37H_2O$ (**2**) in a 50:50 water : acetonitrile mixture, transferred to the gas phase by electrospray ionisation (ESI). These spectra show the presence of key ions in the gas phase; in particular: $\{[(TeO_3)W_3O_9]Na\}^-$ (m/z 894.7); $\{[W_4O_{13}]Na\}^-$ (m/z 966.8); $\{[(TeO_3)W_5O_{15}]Na\}^-$ (m/z 1358.6) and $\{[W_6O_{19}]Na\}^-$ (m/z 1430.6). One of the most important features relates to the presence of one quarter unit of **2** including the TeO_2 linker: $\{[(TeO_3)(TeO_2)W_7O_{25}]H_4Na_4\}^{2-}$ (m/z 1058.6); and also another fragment which can be assigned to one quarter unit of **2** including the TeO_2 linker and pendant TeO_3 : $\{[(TeO_3)W_7O_{25}(TeO_2)(TeO_3)]H_9Na(H_2O)\}^{2-}$ (m/z 1123.6).

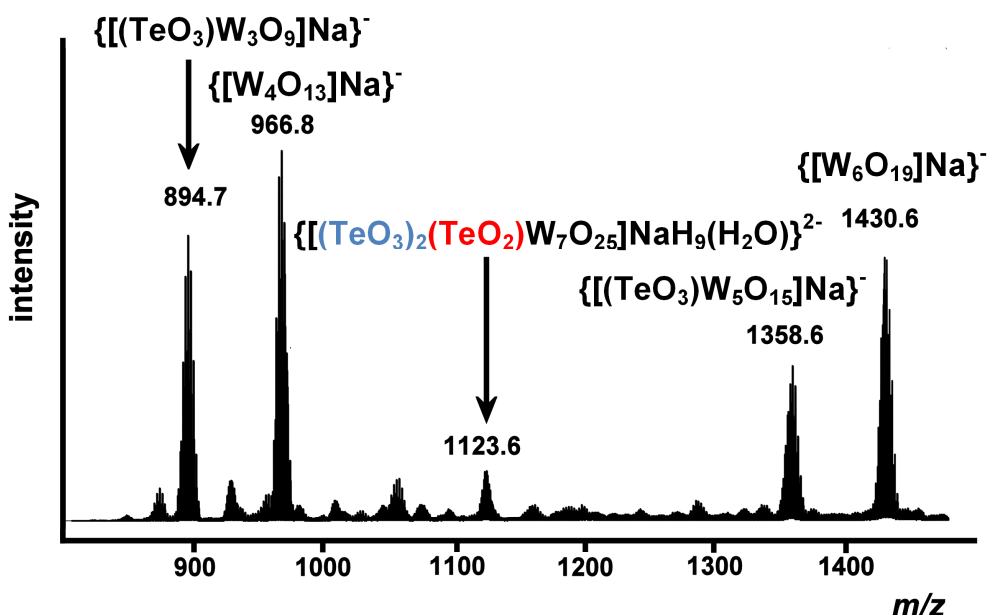


Figure S4.3 Mass Spectra data of $\text{Na}_{28}[\text{W}_{28}\text{Te}_{10}\text{O}_{118}] \cdot 45\text{H}_2\text{O}$ (**3**) in a 50:50 water : acetonitrile mixture, transferred to the gas phase by electrospray ionisation (ESI). The profile of $\text{Na}_{26}[\text{W}_{28}\text{Te}_{9}\text{O}_{115}] \cdot 37\text{H}_2\text{O}$ (**2**) is analogous to that of **3**. These spectra show the presence of key ions in the gas phase; in particular: $\{[(\text{TeO}_3)\text{W}_3\text{O}_9]\text{Na}\}^-$ (m/z 894.7); $\{\text{[W}_4\text{O}_{13}]\text{Na}\}^-$ (m/z 966.8); $\{[(\text{TeO}_3)\text{W}_5\text{O}_{15}]\text{Na}\}^-$ (m/z 1358.6) and $\{\text{[W}_6\text{O}_{19}]\text{Na}\}^-$ (m/z 1430.6). One of the most important features relates to the presence of one quarter unit of **3** including the TeO_2 linker *and* pendant TeO_3 : $\{[(\text{TeO}_3)\text{W}_7\text{O}_{25}(\text{TeO}_2)(\text{TeO}_3)]\text{H}_9\text{Na}(\text{H}_2\text{O})\}^{2-}$ (m/z 1123.6).

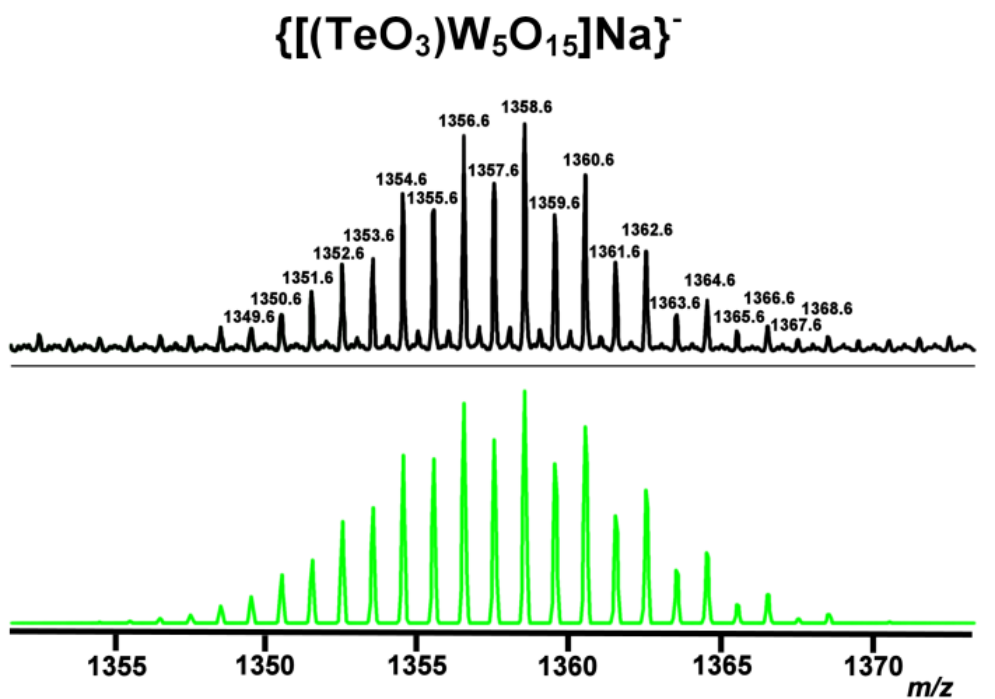


Figure S4.4 Heterohexameric fragment $\{[(\text{TeO}_3)\text{W}_5\text{O}_{15}]\text{Na}\}^-$ (m/z 1358.6) observed in the fragmentation of $(\text{C}_2\text{H}_8\text{N})_6\text{Na}_{18}[\text{W}_{28}\text{Te}_8\text{O}_{112}] \cdot 53\text{H}_2\text{O}$ (1), $\text{Na}_{26}[\text{W}_{28}\text{Te}_9\text{O}_{115}] \cdot 37\text{H}_2\text{O}$ (2) and $\text{Na}_{28}[\text{W}_{28}\text{Te}_{10}\text{O}_{118}] \cdot 45\text{H}_2\text{O}$ (3) in a 50:50 water : acetonitrile mixture. Black line is observed spectra and the green line the simulated m/z envelope.

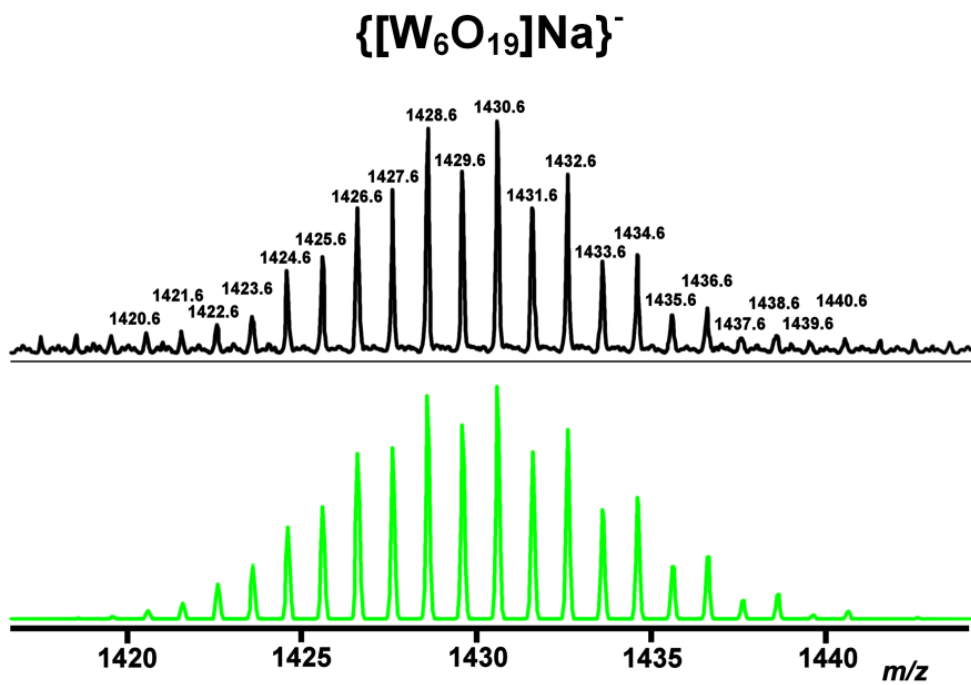


Figure S4.5 A range of singly and doubly charged isopolyanionic species are observed in the fragmentation of all three compounds, $(\text{C}_2\text{H}_8\text{N})_6\text{Na}_{18}[\text{W}_{28}\text{Te}_8\text{O}_{112}] \cdot 53\text{H}_2\text{O}$ (1), $\text{Na}_{26}[\text{W}_{28}\text{Te}_9\text{O}_{115}] \cdot 37\text{H}_2\text{O}$ (2) and $\text{Na}_{28}[\text{W}_{28}\text{Te}_{10}\text{O}_{118}] \cdot 45\text{H}_2\text{O}$ (3), in a 50:50 water : acetonitrile solvent system employed for these mass spectra analyses. The above example is the isohexameric fragment $\{[\text{W}_6\text{O}_{19}]\text{Na}\}^-$ (m/z 1430.6). Black line is observed spectra and the green line the simulated m/z envelope.

Table S2. Assignments for $(C_2H_8N)_6Na_{18}[W_{28}Te_8O_{112}] \cdot 53H_2O$ (**1**)

Negative charge	m/z	Assignment
2	1058.6	$[TeW_7O_{28}(TeO_2)H_4Na_4]^{2-}$
2	978.7	$[TeW_7O_{28}Na_4H_4]^{2-}$
2	899.7	$[W_7O_{26}H_4Na_4]^{2-}$
2	819.8	$[W_7O_{22}]^{2-}$
1	1430.6	$[W_6O_{19}Na]^-$
2	703.8	$[W_6O_{19}]^{2-}$
2	783.8	$[W_6O_{22}HNa_5]^{2-}$
1	1358.6	$[TeW_5O_{18}Na]^-$
1	1336.6	$[TeW_5O_{18}H]^-$
2	666.8	$[W_5O_{20}Na_4H_4]^{2-}$
1	966.8	$[W_4O_{13}Na]^-$
2	471.9	$[W_4O_{13}]^{2-}$
1	894.7	$[TeW_3O_{12}Na]^-$
1	734.8	$[W_3O_{10}Na]^-$
1	712.8	$[W_3O_{10}H]^-$
1	502.9	$[W_2O_7Na]^-$
1	480.9	$[W_2O_7H]^-$

Table S3. Assignments for $\text{Na}_{26}[\text{W}_{28}\text{Te}_9\text{O}_{115}] \cdot 37\text{H}_2\text{O}$ (**2**)

Negative charge	m/z	Assignment
2	1123.6	$[(\text{TeO}_3)\text{W}_7\text{O}_{25}(\text{TeO}_2)(\text{TeO}_3)\text{H}_9\text{Na}(\text{H}_2\text{O})]^{2-}$
2	1058.6	$[\text{TeW}_7\text{O}_{28}(\text{TeO}_2)\text{H}_4\text{Na}_4]^{2-}$
1	1428.6	$[\text{W}_6\text{O}_{19}\text{Na}]^-$
1	1358.6	$[\text{TeW}_5\text{O}_{18}\text{Na}]^-$
1	966.8	$[\text{W}_4\text{O}_{13}\text{Na}]^-$
1	894.7	$[\text{TeW}_3\text{O}_{12}\text{Na}]^-$

Table S4. Assignments for $\text{Na}_{28}[\text{W}_{28}\text{Te}_{10}\text{O}_{118}] \cdot 45\text{H}_2\text{O}$ (**3**)

Negative charge	m/z	Assignment
1	1430.6	$[\text{W}_6\text{O}_{19}\text{Na}]^-$
1	966.8	$[\text{W}_4\text{O}_{13}\text{Na}]^-$
2	819.8	$[\text{W}_7\text{O}_{22}]^{2-}$
2	703.8	$[\text{W}_6\text{O}_{19}]^{2-}$
2	587.9	$[\text{W}_5\text{O}_{16}]^{2-}$
2	502.9	$[\text{W}_4\text{O}_{14}\text{Na}_2]^{2-}$
2	480.9	$[\text{W}_4\text{O}_{14}\text{H}_2]^{2-}$
2	471.9	$[\text{W}_4\text{O}_{13}]^{2-}$
1	1358.6	$[\text{TeW}_5\text{O}_{18}\text{Na}]^-$
2	1058.6	$[\text{TeW}_7\text{O}_{28}(\text{TeO}_2)\text{H}_4\text{Na}_4]^{2-}$
2	1123.6	$[(\text{TeO}_3)\text{W}_7\text{O}_{25}(\text{TeO}_2)(\text{TeO}_3)\text{H}_9\text{Na}(\text{H}_2\text{O})]^{2-}$
2	894.7	$[\text{TeW}_3\text{O}_{122}\text{Na}_2]^{2-}$
3	925.7	$[(\text{TeW}_3\text{O}_{13})_3\text{Na}_5\text{H}_4]^{3-}$

V Electrochemistry

Solid state Cyclic Voltammograms were obtained using a Model Versastat 4 electro analysis system by Princeton Applied Research. The standard three-electrode arrangement was employed with a Pt mesh auxiliary electrode, 1.5 mm glassy carbon working electrode, and Ag/Ag⁺ reference electrode. All potentials are quoted relative to the Ag/Ag⁺ reference electrode. The glassy carbon working electrodes (diameter 1.5 mm) were polished with alumina (3 µm) on polishing pads, rinsed with distilled water and sonicated in H₂O and then acetone solution before each experiment. The cell was purged with Ar for at least 10 minutes before each experiment.

The solid compounds were transferred to the surface of the carbon electrode as follows. An amount of ~10 mg of crystalline material was placed on a coarse grade filter paper and ground uniformly to a microcrystalline size. This powder was then suspended in a dilute acetone (10 mL) solution of polystyrene (1 – 2 mg). A few drops of the suspended solid material added on the surface of the carbon electrode where a POM-styrene thin film formed upon evaporation of the acetone. Then the electrode was immersed in a 10 mL solution of acetonitrile containing 0.1 M tetrabutylammonium tetrafluoroborate. The thin film was stable during the course of the electrochemical study which allowed us to observe the W-centered redox waves. Only after a period of time (30 - 40 min) the solid material gradually detached from the surface of the electrode due to partial dissolution of the polystyrene film in CH₃CN and as a result a dramatic decrease of the intensity was observed. The main characteristic peaks associated with the tungsten centres show a routine motif. The redox couples appeared broadened and as a result made the accurate calculation of the typical CV parameters extremely difficult. Studying the compounds **1** to **3**, in the region of negative potential values from 0 to -2000 mV, the W-centered redox waves are shifted towards more negative values since the introduction of additional [TeO₃]²⁻ units increases the overall negative charge of the cluster and consequently makes the reduction of the W centers harder.

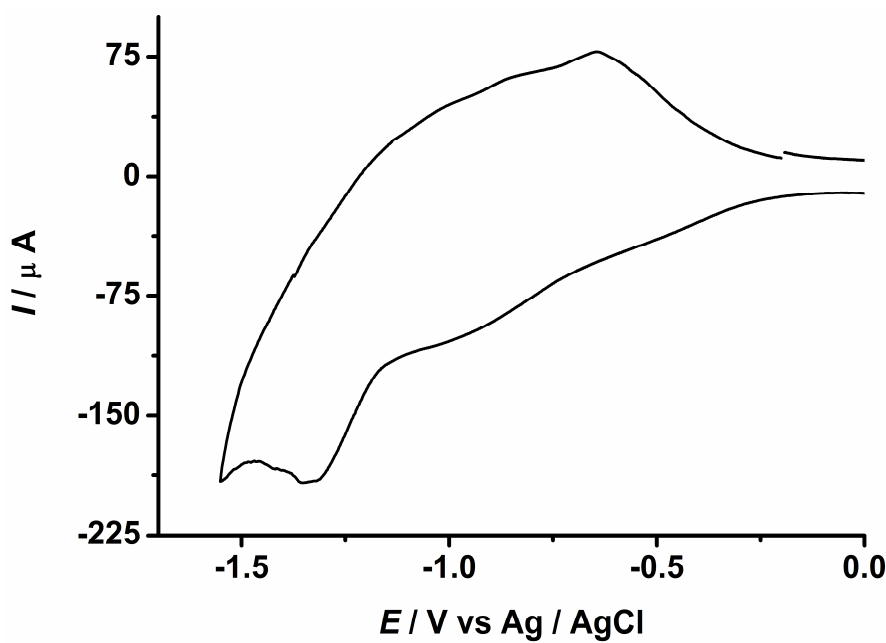


Figure S5.1 Cyclic voltammograms of compound **1** immobilized on the surface of the GC electrode, in 0.1 M TBABF₄ acetonitrile solution. The scan rate was 100 mV s⁻¹, the working electrode was glassy carbon (1.5 mm) and the reference electrode was Ag/Ag⁺.

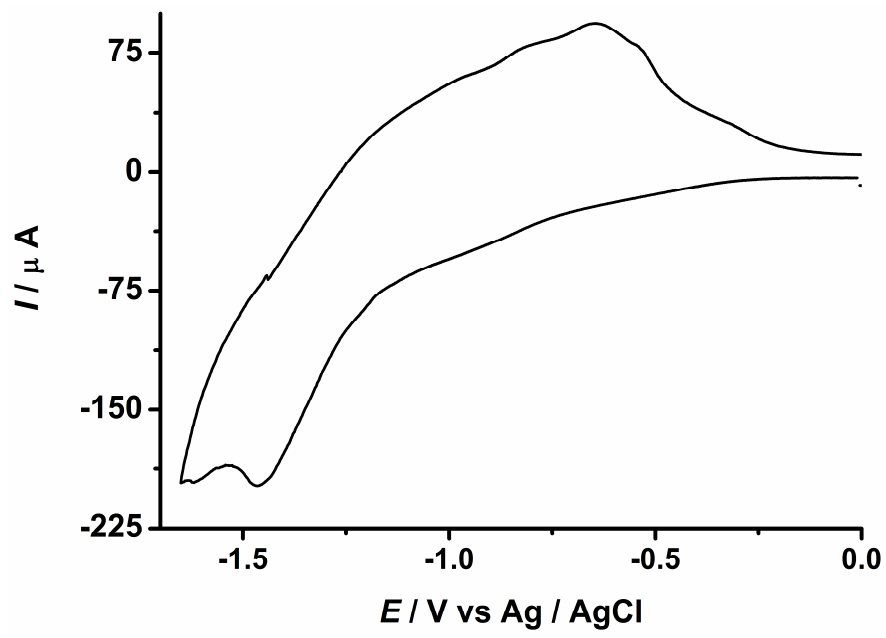


Figure S5.2 Cyclic voltammograms of compound **2** immobilized on the surface of the GC electrode, in 0.1 M TBABF₄ acetonitrile solution. The scan rate was 100 mV s⁻¹, the working electrode was glassy carbon (1.5 mm) and the reference electrode was Ag/Ag⁺.

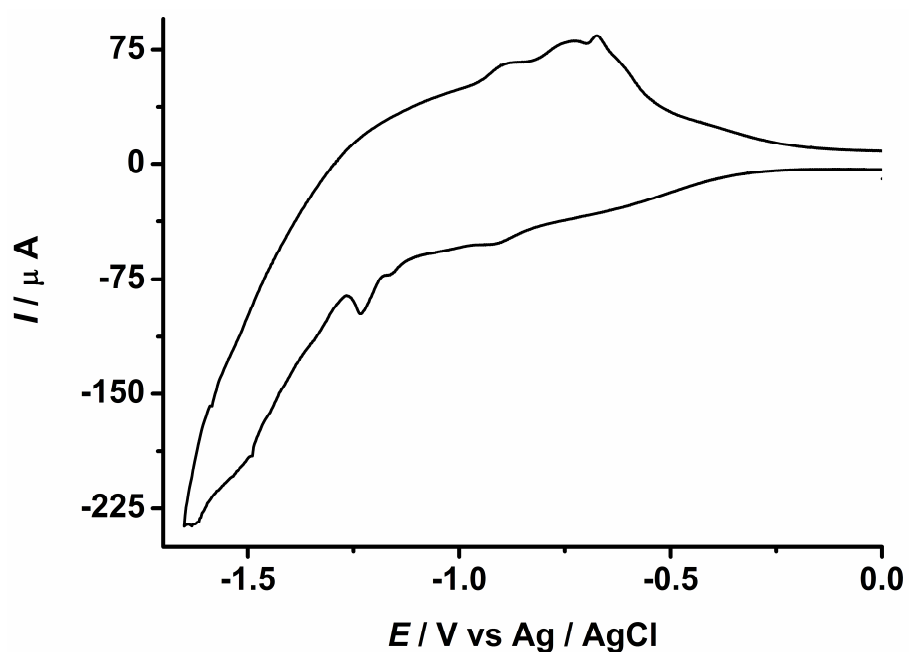


Figure S5.3 Cyclic voltammograms of compound **3** immobilized on the surface of the GC electrode, in 0.1 M TBABF₄ acetonitrile solution. The scan rate was 100 mV s⁻¹, the working electrode was glassy carbon (1.5 mm) and the reference electrode was Ag/Ag⁺.

VI IR Spectra

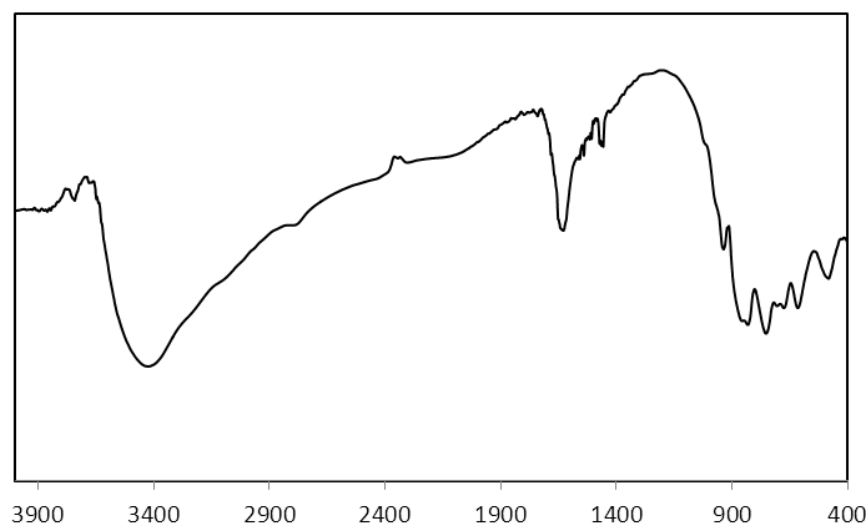


Figure S6.1 IR spectrum of (C₂H₈N)₆Na₁₈[W₂₈Te₈O₁₁₂]•53H₂O (1)

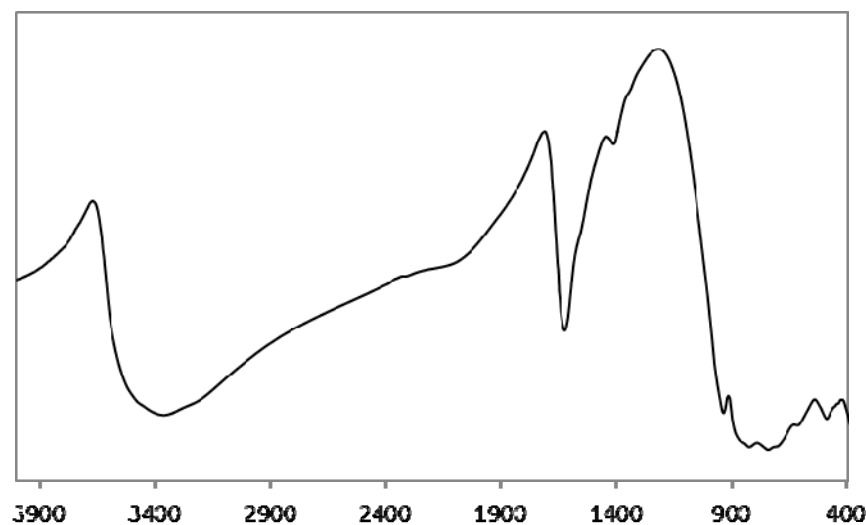


Figure S6.2 IR spectrum of Na₂₆[W₂₈Te₉O₁₁₅]•37H₂O (2)

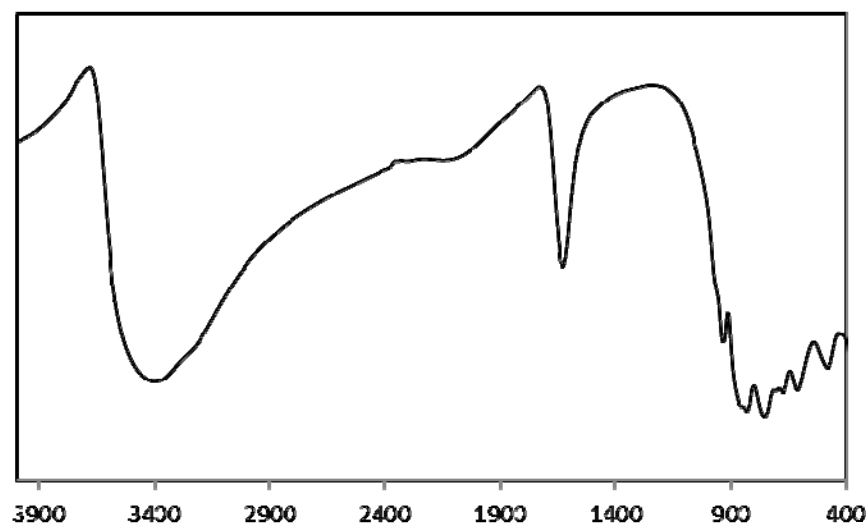


Figure S6.3 IR spectrum of Na₂₈[W₂₈Te₁₀O₁₁₈]•45H₂O (3)